Photochemical & Photobiological Sciences (2023) 22:1945–1959
https://doi.org/10.1007/s43630-023-00423-3

ORIGINAL PAPERS

Protective effect and mechanism research of *Phyllanthus emblica Linn.* fruit extract on UV-induced photodamage in keratinocytes

Liping Qu[1,2,3] · Feifei Wang[1,2,3] · Yueyue Chen[1]

Received: 19 January 2023 / Accepted: 10 April 2023 / Published online: 19 April 2023

Abstract
Ultraviolet (UV) irradiation causes acute and chronic cutaneous effects that may result in photodamage and photoaging. Epidermis keratinocytes, as the closest surface of skin, are susceptible to damage from UV rays. *Phyllanthus emblica Linn.* fruit (PE) extract, as a medicine and food dual-use plant, contains high levels of polyphenols and possesses multiple pharmacological properties. The present study investigated common and different molecular mechanisms and signaling pathway activations of UVA and UVB stimulated cell damage and photoprotective effect of PE extract against UVA and UVB by Methyl Thiazolyl Tetrazolium (MTT) method, Elisa assay, flow cytometry, differentially expressed genes analysis and western blot analysis. The results showed that UVA exposure (10 J/cm^2) reduced HaCaT cell viability significantly, increased the apoptosis rate, elevated intracellular reactive oxygen species level and reduced antioxidant enzyme activities. And UVA irradiation could inhibit the ERK/TGF-β/Smad signaling pathway to downregulate collagen I, collagen III and elastin expressions, resulting in the photoaging of skin cells. We also found UVB exposure (30 mJ/cm^2) caused HaCaT cell damage, promoted apoptosis, increased ROS production and induced the release of proinflammatory cytokines (IL-1α, IL-6 and PGE2). Further, in HaCaT cells, UVB ray was able to induce the activation of apoptosis markers (cleaved PARP1 and cleaved caspase3) through the MAPK/AP-1 signaling pathway using western blot analysis. Pre-treatment of PE extract prevented the UVA and UVB induced photoaging and injury in HaCaT cells through activation of ERK/TGF-β/Smad pathway and inhibition of MAPK/AP-1 pathway, respectively. Therefore, PE extract has the potential to be used as an oral and topical preparation against skin aging and injury induced by UVA and UVB.

Keywords Ultraviolet radiation · Human keratinocytes · Photoaging · Photoprotection · *Phyllanthus emblica Linn.*

1 Introduction

In recent years, climate change and environmental pollution have exacerbated the destruction of the ozone layer in the atmosphere, resulting in an increase of UV radiation reaching the earth's surface [1]. Furthermore, there has been a dramatic increase in the incidence of skin aging and skin diseases due to excessive skin exposure to UV radiation. UV radiation can be divided into the following three types: UVA, UVB, and UVC, which cover the regions of 315 and 400 nm, 280 and 315 nm, and 200 and 280 nm, respectively. UVC has the weakest penetration, being almost entirely blocked by the ozone layer. The penetration of UVB is greater than UVC, but 95% of UVB can be absorbed by the ozone layer, with only a small amount reaching the ground [2]. UVA, which has a longer wavelength, has the strongest penetration power, with 95% of UVA reaching the ground through clouds and ozone. At the same dose, UVB has a stronger damage effect than UVA. However, UVA makes up a large majority of solar UV radiation and poses a comparable risk to UVB (5%) [3].

UVB can reach the epidermis and superficial dermis, resulting in direct damage to the skin. UVB is readily absorbed by DNA, subsequently leading to production of

✉ Yueyue Chen
chenyueyue@winona.cn

1 Innovation Materials Research and Development Center, Botanee Research Institute, Shanghai Jiyan Bio-Pharmaceutical Development Co., Ltd., Shanghai 201702, China

2 Yunnan Characteristic Plant Extraction Laboratory, Yunnan Yunke Characteristic Plant Extraction Laboratory Co., Ltd., Kunming 650106, China

3 Yunnan Botanee Bio-Technology Group Co., Ltd., Kunming 650106, China

6–4 photoproducts (6–4 PP) and cyclobutene pyrimidine dimers (CPD), DNA strand breaks and crosslinks [4]. At the same time, UVB-induced ROS can cause irreversible damage to biomacromolecules such as DNA, proteins and lipids. Therefore, the structural integrity of the skin and bioactivities of cells are disrupted by UVB induced changes, leading to oxidative stress, inflammatory injury and apoptosis, and even carcinogenesis through long-term exposure to UVB [5].

In addition, skin photoaging is heavily affected by UVA radiation. There are two following different types of skin aging: extrinsic aging (photoaging) and intrinsic aging [1]. Due to its greater penetration power, UVA can penetrate deeply to the basal layer of the epidermis and dermis and induce cell damage and photoaging associated with reactive oxygen species (ROS) excess production. In the normal skin tissues, synthesis and breakdown of the extracellular matrix (ECM)-related molecules such as type I, III, and IV collagen, fibronectin, elastin, laminin and proteoglycans are in dynamic equilibrium, contributing to the maintenance of skin structure, elasticity, and resilience. The family of matrix metalloproteinases (MMPs) acts as the collagenolytic enzyme and is responsible for the breakdown of extracellular matrix components that contribute to skin aging. Study has shown that UVA-induced ROS promote expression of MMPs [6]. As a result, both UVA and UVB irradiation induce oxidative stress and inflammation, which disrupt the skin barrier and create wrinkles in the skin, resulting in skin injury. As the outermost barrier of the skin, human keratinocytes are the primary targets of UV radiation. Exploring the different mechanisms of UVA and UVB-induced photodamage of keratinocytes may develop strategies for the prevention and treatment of skin diseases associated with UV-ray radiation.

Our previous study demonstrated, through a combination of transcriptomic and proteomic analyses, that different and similar changes in gene transcription or protein abundances occurred after UVA and UVB irradiation [7]. However, detailed molecular mechanisms and signaling pathway activations of UVB and UVA induced cell damage are needed for further in-depth investigation.

Physical and chemical sunscreens are restricted substances that have certain negative effects on the human body and the environment [8]. Finding safe and biodegradable natural substances for resisting UV is a hot research topic. Meanwhile, oral photoprotection may be an essential method for providing additional sun protection to humans [9]. A great number of studies demonstrated that some plant extracts such as Gastrodia elata Blume, Poria cocos Wolf, Cocoa and Polypodium leucotomos extract, given orally every day, may be efficient in preventing skin injury by exhibiting photoprotective effects [10–12]. *Phyllanthus emblica Linn.* (PE), family *Euphorbiaceae*, whose common name is Yunnan Olive, amla or Indian gooseberry, is widespread throughout the subtropical and tropical areas of China, Indonesia, and India. The fruit of PE is a medicine and food dual-use plant, is sweet, sour and astringent in flavor and slightly cool, and it acts on the lung and stomach meridians. PE is rich in polyphenols, vitamins, polysaccharides, amino acids and alkaloids with pharmacological activities such as slaking thirst, digestion, anti-inflammation, antioxidant, anti-tumor and anti-lipidemic. Polyphenols display the prominent antioxidant activity among all active ingredients of PE. In the previous study, the anti-inflammatory and anti-apoptotic effects of PE exposed to UVB were reported [13]. However, the corresponding mechanism and signaling pathway of PE against photodamage induced by UVA and UVB have not been investigated. Therefore, in the present study, we investigated the photoprotective effect and the corresponding mechanism of PE in keratinocytes against UVA and UVB.

2 Materials and methods

2.1 Chemicals and reagents

The preparations and assays were conducted using ultrapure water with Milli-Q IX 7005 water purification system (Merck, Darmstadt, Germany). Dulbecco's Modified Eagle's Medium (DMEM), Trypsin–EDTA solution and Fetal Bovine Serum (FBS) were obtained from Gibco (USA). Phosphate Salt Buffer (PBS), gallic acid standard, folin phenol, sodium carbonate, phosphoric acid and acetonitrile were all purchased from Sigma-Aldrich (St. Louis, MO, USA).

2.2 Plant material

PE was collected in October 2020 from Kunming, Yunnan Province, China and identified by Professor Haiyang Liu (based on permission No. 2020-10 from Kunming Institute of Botany, Kunming, China). PE, as a voucher specimen (No. 20201012), has been deposited in in the herbarium of Botany Research Institute, Shanghai Jiyan Bio-Pharmaceutical Development Co. Ltd., Shanghai, China.

2.3 Preparation of PE extract

Clean and dry PE was crushed into powder by a versatile plant pulverizer and sieved through a 6-mesh sieve. 100 g of PE powder was accurately weighed and added to 1000 ml of 70% ethanol solution. Then PE was extracted twice times at 60 °C for 2 h with reflux. The filtrate was combined and concentrated with a hypobaric drying method. Then the concentrate was freeze-dried to powder. The yield of PE extract was 61.23%.

2.4 The total polyphenols content of PE extract

The total polyphenols content of PE extract was determined by the Folin-Ciocalteu method. The gallic acid standard was weighed 0.0025 g accurately, transferred into a 20 ml volumetric flask and dissolved with ethanol, as standard solution. The gallic acid standard solution was diluted in ethanol using the doubling method. 0.5 ml of gallic acid standard solution of different concentrations was pipetted into a 10 ml volumetric flask. Then 5 ml of 10% folin phenol solution was added. The mixture was shaken well and left for 5 min. 10% sodium carbonate solution was added and fixed the volume to the calibration line. And the mixture was allowed to rest for 1 h, protected from light. The absorbance value was measured at a wavelength of 740 nm by a microplate reader (Multiskan Sky, Thermo Fisher Scientific, USA). A standard curve of the gallic acid was developed using the absorbance value as a vertical coordinate and the concentration of the gallic acid (mg/ml) as a horizontal coordinate. The calibration curve was linear over the gallic acid concentration range 0.0–0.125 mg/ml and found to be $Y = 0.0319X - 0.0027$, $R^2 = 0.9902$ (see Supplement Fig. 1A). 0.5 ml of PE extract (0.1 mg/ml) was taken in a 10-ml volumetric flask and the absorbance was measured as described.

2.5 The gallic acid content of PE extract

The gallic acid content was measured with an Agilent 1260 high-performance liquid chromatograph (HPLC) (Agilent, Palo Alto, CA, USA). The gallic acid standard was accurately weighed, transferred into a 20-ml volumetric flask by adding ethanol to scale and sonicated to dissolve. At the same time, an appropriate amount of PE extract was weighed, placed into a 20 ml volumetric flask, and dissolved. The gallic acid standard solution and PE extract were filtered with a 0.22 μm filter membrane. Then the gallic acid standard solution was diluted in ethanol using the doubling method. The samples were injected into HPLC for analysis, making injection volumes of 10 μl. The standard curve was drawn with the standard concentration as the ordinate and the peak area as the abscissa.

The parameters for HPLC analysis were as follows: Chromatographic separations were carried out at 30 °C on an Agilent ZORBAX SB-AQ column, 4.6 × 250 mm i.d., 5 μm particle size with UV detection at 270 nm. Mobile phases were composed of 0.1% phosphoric acid in water (mobile phase A) and 100% acetonitrile (mobile phase B). Elution condition was employed according to the following program: 90% eluent A; 10% eluent B. The HPLC flow rate was 1 ml/min, and the run time was 10 min. The linear regression equation $Y = 28.477X - 8.4814$ ($R^2 = 0.9994$) proved that the gallic acid concentration was linear, with a peak area in the range of 6.55–209.60 μg/ml (see Supplement Fig. 1B). The PE extract was injected into HPLC for gallic acid analysis. Chromatographic peaks of PE extract were identified by comparing its retention time with pure standard (see Supplement Fig. 1C).

2.6 Cells culture and UV treatment

Immortalized human keratinocytes (HaCaT) were purchased from Cell Resource Center (Wuhan, China). The HaCaT cells were cultured in DMEM contained 10% FBS at 37 °C in a 5% CO_2 incubator. When cells were grown to 70% confluency, they were exposed to UV radiation. UV-irradiation was performed with a 3T3 NRU phototoxicity irradiation system (HOPE-MED 8130GT, Tianjin Hope Industry and Trade Co., Ltd, China) containing the following two different kinds of lamps: four UVA lamps (350–400 nm, peak emission $\lambda = 365$ nm) at a dose-rate of 2 mW/cm^2 and four UVB lamps (280–320 nm, peak emission $\lambda = 310$ nm), which were controlled at a dose-rate of 0.5 mW/cm^2. The intensity of the lamps was measured using a UV meter (Tianjin Hope Industry and Trade Co., Ltd, China) with UVA and UVB detector.

The concentration of PE (50, 100 and 200 μg/ml) was selected based on 90% cell viability measured by the Methyl Thiazolyl Tetrazolium (MTT) assay (see Supplement Fig. 2). The PE group cells were incubated in serum-free medium for two hours at 37 °C with different concentrations of the PE extract. Then, the medium was removed, and cells were washed twice with cold PBS. After that it was added a thin layer of PBS containing different concentrations of the PE extract to expose the cells at different doses to UVA or UVB radiation (10 ml was used in 10 cm cell culture dishes, 100 ul in 96-well plates and 2 ml in 6-well plates). The UVA group or UVB group cells were irradiated with 10 J/cm^2 of UVA or 30 mJ/cm^2 UVB, respectively. The blank control sample was treated in the same way, avoiding exposure to radiation. Assays were performed immediately after UV irradiation, when not defined.

2.7 Cell proliferation activity assay

The cell proliferation activity was measured using the CCK8 kit (Dojindo Molecular Technologies, Shanghai, China). HaCaT cells were pre-treated with the PE extract (50, 100 and 200 μg/ml) for 2 h. After the pre-treatment, PBS was replaced immediately by the complete medium. Then the cells were exposed to 10 J/cm^2 of UVA and 30 mJ/cm^2 of UVB radiations, respectively. Further, samples were incubated at 37 °C, 5% CO_2, for 24 h. Then, 10 μl of CCK8 reagent was added to all cell samples. After another 2 h in the cell culture incubator, the sample absorbance was determined at 450 nm by the microplate reader.

2.8 Apoptosis analysis

The apoptosis analysis was measured using the Annexin V-FITC Cell Apoptosis Kit (Beyotime Biotechnology, Shanghai, China). HaCaT cells were harvested and resuspended in 195 μL of staining buffer after incubation for 24 h. After that, cells were incubated for 20 min in the dark with 5 μL of Annexin V-FITC and 10 μL of propidium iodide (PI). A BD FACSVerse™ flow cytometer (BD Biosciences, San Jose, CA, USA) was used to analyze early apoptosis and necrosis cells.

2.9 Measurement of intracellular ROS generation

The intracellular ROS level was measured using the ROS Assay Kit (Beyotime Biotechnology, Shanghai, China). After incubation for 24 h, the culture medium was removed, 10 μM of DCFH-DA fluorogenic probe was added and incubated in a light protective 37 °C incubator for 20 min. Then cell samples were washed with serum-free medium for three times and measured by flow cytometry. DCFH-DA itself has no fluorescence and can freely cross the cell membrane. After entering the cell, it can be hydrolyzed by the esterase in the cell to generate DCFH. Intracellular DCFH can be oxidized to DCF by ROS. DCF has strong green fluorescence, so the change of ROS level can be observed indirectly by detecting the fluorescence intensity of DCF.

2.10 Measurement of proinflammatory factors

The proinflammatory factors IL-1α and IL-6 were measured strictly according to the specification of the ELISA Kits (Proteintech, Wuhan, China). A PGE2 ELISA Kit (Cayman Chemicals, MI, USA) was used to measure serum PGE2 production. After incubation for 24 h, the supernatant was collected and centrifuged at 10,000*g* for 20 min. The relative IL-1α, IL-6 and PGE2 releases were calculated using ELISA kits according to the manufacturer's protocol.

2.11 Quantitative RT-PCR assay

After incubation for 24 h, the cells were washed and collected for RNA analysis. For quantitative real time PCR (qRT-PCR), RNA was extracted from HaCat cells using the GeneJET™ RNA Purification Kit (Thermo Fisher Scientific, USA). RNA isolated from cultured cells was reverse transcribed using the PrimeScript™ RT Master Mix (Takara Bio Inc., Japan) according to the manufacturer's protocol. PCR amplifications were performed using the FastStart Essential DNA Green Master (Roche Diagnostics GmbH, Germany) and a Light cycler® 480 instrument (Roche, USA). The primers used for qRT-PCR were as follows in Supplement Table 1. ACTINB was used as an internal control. The indicated gene expression was calculated according to the $2^{-\Delta\Delta Ct}$ method.

2.12 Western blot assay

After incubation for 24 h, the cells were washed twice with cold PBS and lysed with a cell lysate (Beyotime Biotechnology, Shanghai, China) to prepare a cell lysate at 4 °C. Protein concentration was measured using Enhanced BCA Protein Assay Kit (Beyotime Biotechnology, Shanghai, China) and equal amounts of protein for each sample were separated by SDS-PAGE. Proteins were transferred to PVDF membranes (Millipore, Burlington, MA, USA). TBST (Tanon Life Science, Shanghai, China) was used for washing and 10% milk powder (BBI Life Sciences Corporation, China) in TBST for blocking. The membranes were probed with specific primary antibodies, and further treated with the corresponding HRP-conjugated secondary antibodies. Proteins were then visualized with Chemistar™ High-sig ECL Western Blotting Substrate (Tanon Life Science, Shanghai, China), recorded by Tanon-5200 Chemiluminescent Imaging System (Tanon Life Science, Shanghai, China) and analyzed with Image J software.

2.13 Statistical analysis

All data were based on three independent experiments. Data were expressed as mean ± SD using GraphPad Prism 7 (GraphPad Software, Inc., CA, USA). Statistical comparisons between different treatments were performed using a one-way analysis of variance (ANOVA) and Student's t-tests. When comparing irradiated group with blank control group, significance is indicated by #, P value < 0.05 is indicated as #, P value < 0.01 is indicated as ##; P value < 0.001 is indicated as ###; when comparing sample group with irradiated group, significance is indicated by *, P value < 0.05 is indicated as *, P value < 0.01 is expressed as **, P value < 0.001 is expressed as ***.

3 Results

3.1 Total polyphenols and gallic acid in PE extract

Polyphenols are known to have antioxidative, anti-carcinogenic and anti-inflammatory properties. Gallic acid is a polyphenolic secondary metabolite of a variety of plants [14]. To identify the compounds responsible for the antioxidant and anti-inflammatory properties of PE, the content of plant phenolic compounds and gallic acid were measured. The total polyphenols content in PE was 41.61 ± 1.82%. Supplement Fig. 1C shows the HPLC fingerprints of the PE extract and gallic acid, indicating that gallic acid was the

most prominent phenolic substance in PE extract, with a content of 2.15 ± 0.11%.

3.2 Photoprotective effect of PE extract against the UV-induced injury

As shown in Fig. 1A, the number of HaCat cells was significantly reduced compared to the blank group, and the cell morphology significantly became shrunken and rounded by UVA and UVB irradiation. There was no significant change in cell morphology and no apparent cell death with 200 μg/ml of PE extract pre-treatment. The cell viabilities of the UVA and UVB irradiation groups were significantly lower than the blank group, showing that UVA (10 J/cm^2) and UVB (30 mJ/cm^2) irradiation can cause cell injury and death (Fig. 1B). Pre-treatment (2 h) with 50, 100 and 200 μg/ml of PE extract before the irradiation led to a significant increase of the HaCaT cell viability after UVA and UVB exposure. This suggested that PE extract had a favorable protective effect against cell damage induced by UVA and UVB radiation.

3.3 Photoprotective effect of PE extract against the UV-induced apoptosis

Prolonged exposure of cells or tissues to UV light can cause cellular damage or death. Flow cytometry analysis revealed that the apparent increase by both UVA and UVB irradiation in the percentage of late apoptotic and necrotic cells (Annexin V-FITC and PI double positive), compared with those of un-irradiated HaCaT cells (Fig. 2). Pre-treatment with PE extract (50, 100 and 200 μg/ml) remarkably decreased the proportions of these two types of cells as dose increased. For example, the proportion of late apoptotic cells was reduced from 24.4% in UVA-irradiated group to 9.3% in 200 μg/ml of the PE-treated group ($P \leq 0.001$). And the percentage of late apoptotic cells was decreased from 25.4% in UVB-irradiated group to 12.7% in 200 μg/ml of the PE-treated group ($P \leq 0.01$). Based on Fig. 2, the percentages of early apoptotic cells (Annexin V-FITC positive and PI negative) exposed to UVA and UVB respectively were 14.9% and 24.1%, indicating that UVB ray rendered HaCaT cells more vulnerable to apoptosis than UVA ray. It has been shown that PE extract can significantly alleviate the apoptosis and necrosis of cells induced by UVA and UVB.

3.4 Photoprotective effect of PE extract against the UV-induced oxidative stress

It has been previously reported that UV light induces ROS production [15]. ROS levels were determined as oxidative stress. And UV-induced ROS generation plays a crucial role in the photoaging of skin [16]. As shown in Fig. 3A, UV-irradiated HaCat cells exhibited a significant increase in ROS production levels compared to the blank group; however, PE extract (50, 100 and 200 μg/ml) significantly inhibited the intracellular ROS production in UVA-irradiated HaCaT cells. 200 μg/ml of PE extract can scavenge

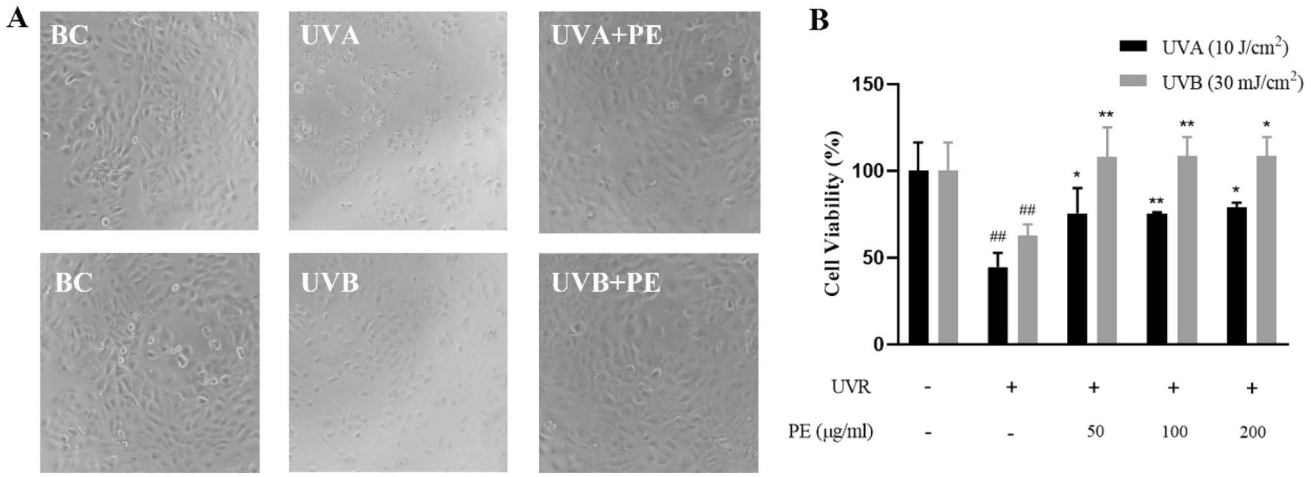

Fig. 1 The photoprotective effect of PE extract against UVA and UVB induced injury in HaCat cells. **A** Representative microphotographs of HaCaT cells taken under the inverted microscope, 100×. 10 J/cm^2 of UVA and 30 mJ/cm^2 of UVB irradiation in HaCaT cells are respectively abbreviated as "UVA" and "UVB". Pre-treatment with 200 μg/ml of PE extract for 2 h, and then irradiation with 10 J/cm^2 of UVA and 30 mJ/cm^2 of UVB in HaCaT cells are respectively abbreviated as "UVA + PE" and "UVB + PE". **B** The cell viability determined by the CCK-8 assay at 24 h after UVA exposure (10 J/cm^2), UVB exposure (30 mJ/cm^2) and pre-treatment with the different concentrations of PE extract. Results are presented as a percentage of cell survival compared to a negative control (–, 100%) before any stress. Significant differences were based on a one-way analysis of variance (ANOVA) and two-detailed *T*-test $^{\#\#}P < 0.01$ with respect to the blank group and $^{*}P < 0.05$ and $^{**}P < 0.01$ with respect to UVR exposure group

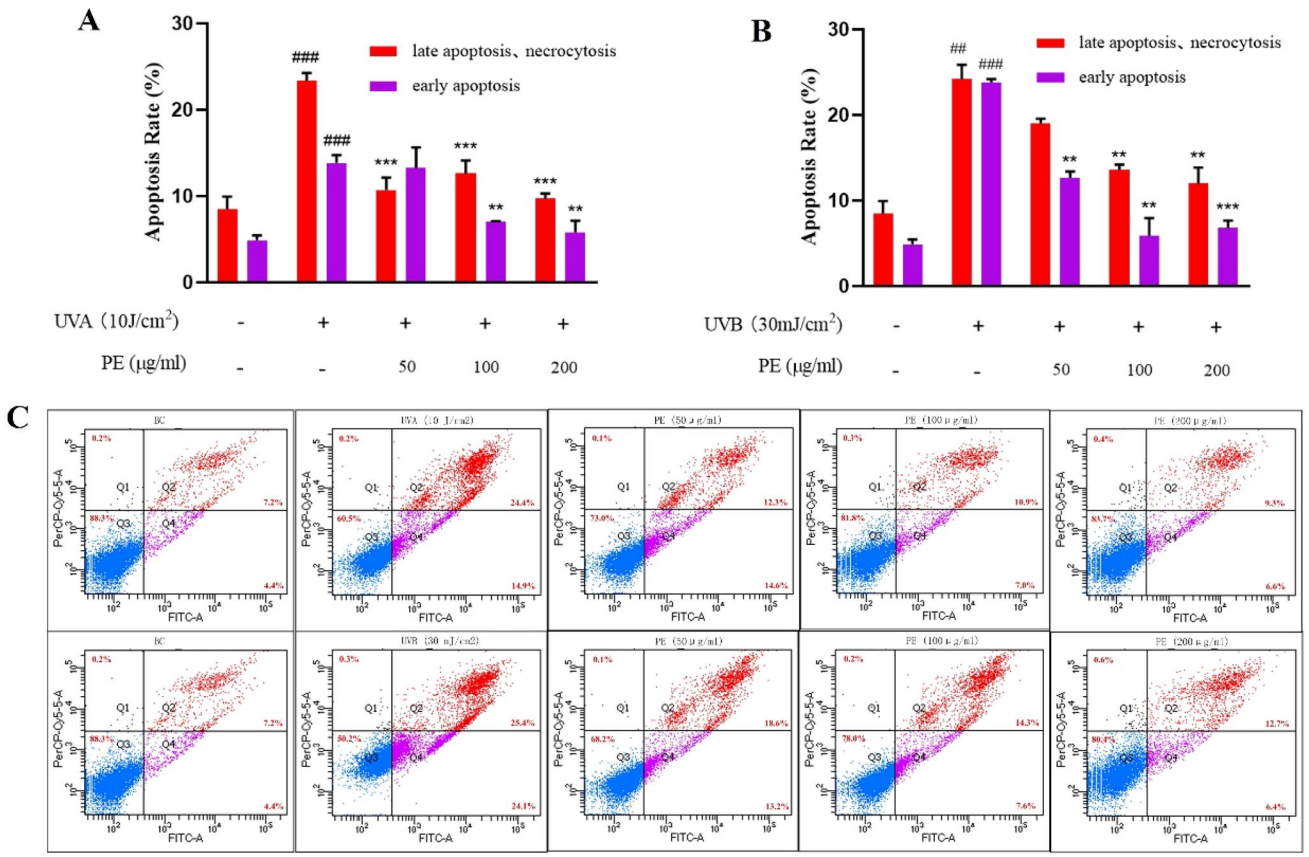

Fig. 2 The photoprotective effect of PE extract against UVA and UVB induced apoptosis in HaCat cells. **A** The percentage of late apoptotic, necrotic HaCaT cells and early apoptotic HaCaT cells detected with a flow cytometry after UVA exposure (10 J/cm^2) and pre-treatment with the different concentrations of PE extract. **B** The percentage of late apoptotic, necrotic HaCaT cells and early apoptotic HaCaT cells were detected with a flow cytometer after UVB exposure (30 mJ/cm^2) and pre-treatment with the different concentrations of PE extract. **C** Effect of PE extract pre-treatment (50, 100 and 200 μg/ml, 2 h) on UVA (10 J/cm^2) and UVB (30 mJ/cm^2) induced apoptosis and detected with a flow cytometry. FITC-A in X axis means the area of FITC fluorescence signal, and FITC-A in Y axis means the area of PI fluorescence signal. Upper left quadrant: necrotic cells; upper right quadrant: late apoptotic cells; lower left quadrant: negatively stained for annexin V and PI (viable cells); lower right quadrant: early apoptotic cells. Significant differences were based on a one-way analysis of variance (ANOVA) and two-detailed *T*-test $^{\#\#}P<0.01$ and $^{\#\#\#}P<0.001$ with respect to the blank group and $^{**}P<0.01$ and $^{***}P<0.001$ with respect to UVR exposure group

the ROS, which is generated by UVB irradiation in HaCaT cells. Therefore, the protection of PE extract against UVA and UVB might be due to their ability to scavenge ROS in the cells.

Superoxide dismutase (SOD) and heme oxygenase 1 (HO-1), as the endogenous anti-oxidases, maintain the balance of redox state and protect cells by scavenging the excessive ROS [17]. Therefore, western blot analysis was performed to further explore the antioxidative effect of PE extract in HaCaT cells. As illustrated in Fig. 3B–D, UVA irradiation decreased the expression of proteins HO-1 and SOD1, which were reversed by the PE extract. However, it was found that UVB radiation did not significantly affect the expression of oxidative enzymes in our study.

3.5 Protective effect of PE extract against the UV-induced inflammation

The releases of proinflammatory cytokines, such as IL-1α, IL-1β, IL-6, and TNF-α, play a crucial role in human inflammatory responses and inflammatory diseases [18]. Prostaglandin E2 (PGE2) is commonly synthesized at low level, but increases significantly in skin squamous cell carcinoma, skin inflammatory conditions such as sunburn and aging skin. PGE2 modulates classic signs of inflammation, including redness and painful swelling [19]. As shown in Fig. 4, the relative expression of IL-1α in HaCaT cells was significantly increased after UVA and UVB irradiation, and 100 μg/ml and 200 μg/ml of

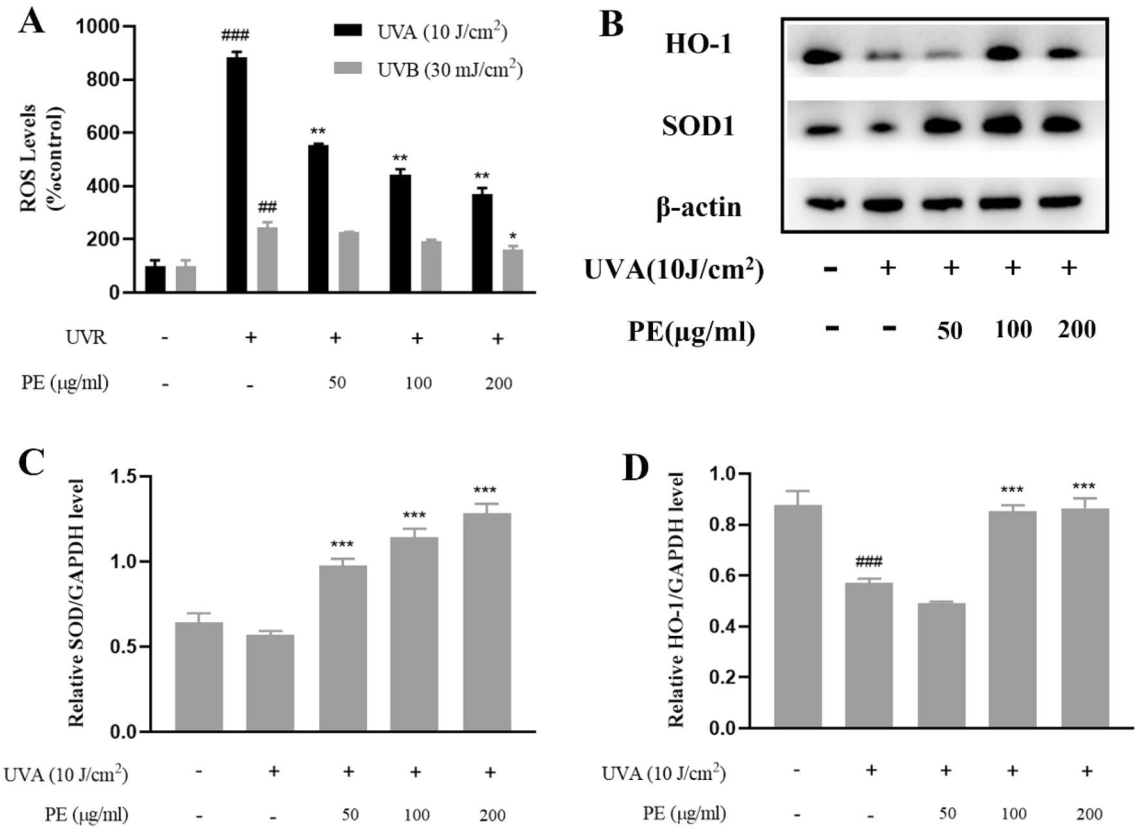

Fig. 3 The photoprotective effect of PE extract against the UVA and UVB induced oxidative stress in HaCaT cells. **A** The intracellular ROS production after UVA (10 J/cm^2) and UVB exposure (30 mJ/cm^2) and pre-treatment with the different concentrations of PE extract was determined by the DCFH-DA method using a flow cytometry. The western blot image analysis (**B**) and relative activation analysis (**C** and **D**) of antioxidant enzyme related proteins (HO-1 and SOD1) after UVA (10 J/cm^2) exposure and pre-treatment with the different concentrations of PE extract were measured by western blot assay. Significant differences were based on a one-way analysis of variance (ANOVA) and two-detailed *T*-test $^{\#\#\#}P<0.001$ with respect to the blank group and $^{***}P<0.001$ with respect to UVR exposure group

PE extract could effectively reduce the increase of IL-1α. After UVB irradiation, the relative expression of IL-6 and PGE2 in HaCaT cells was significantly elevated, which were decreased after PE extract pre-treatment. Simultaneously, no significant changes in the IL-6 and PGE2 contents were observed induced by UVA (Fig. 4B, C). It showed that UVB irradiation could significantly cause the proinflammatory cytokines (IL-1α, IL-6, PGE2) rise and upregulate the inflammatory response. Besides, the levels of inflammatory factors were remarkably reduced after pre-treatment of PE extract.

The expression of cyclooxygenase-2 (COX-2) modulates the synthesis of PGE2 [20]. COX-2 expression level in HaCaT cells was examined using western blot (Fig. 4D). The results showed that UVB irradiation markedly resulted in a rise of COX-2 in HaCaT cells, while PE pre-treatment significantly reduced COX-2 production.

3.6 Mechanism research of UVA and UVB induced HaCaT damage

Based on our previous study [21], we performed multi-omics to characterize the common and different changes in gene transcription after UVB and UVA exposure. Through differentially expressed genes (DEGs) analysis of HaCaT cells induced by UVA and UVB, gene transcription significantly regulated by UVA and UVB radiation was defined as "TCG"; gene transcription specifically regulated by UVB radiation was defined as "TBG"; UVA radiation specific regulated gene transcription is defined as "TAG". Based on these results, it was suggested that a common and differential molecular mechanism might be responsible for cellular damage caused by UVB and UVA exposure. The hub DEGs in each group were listed

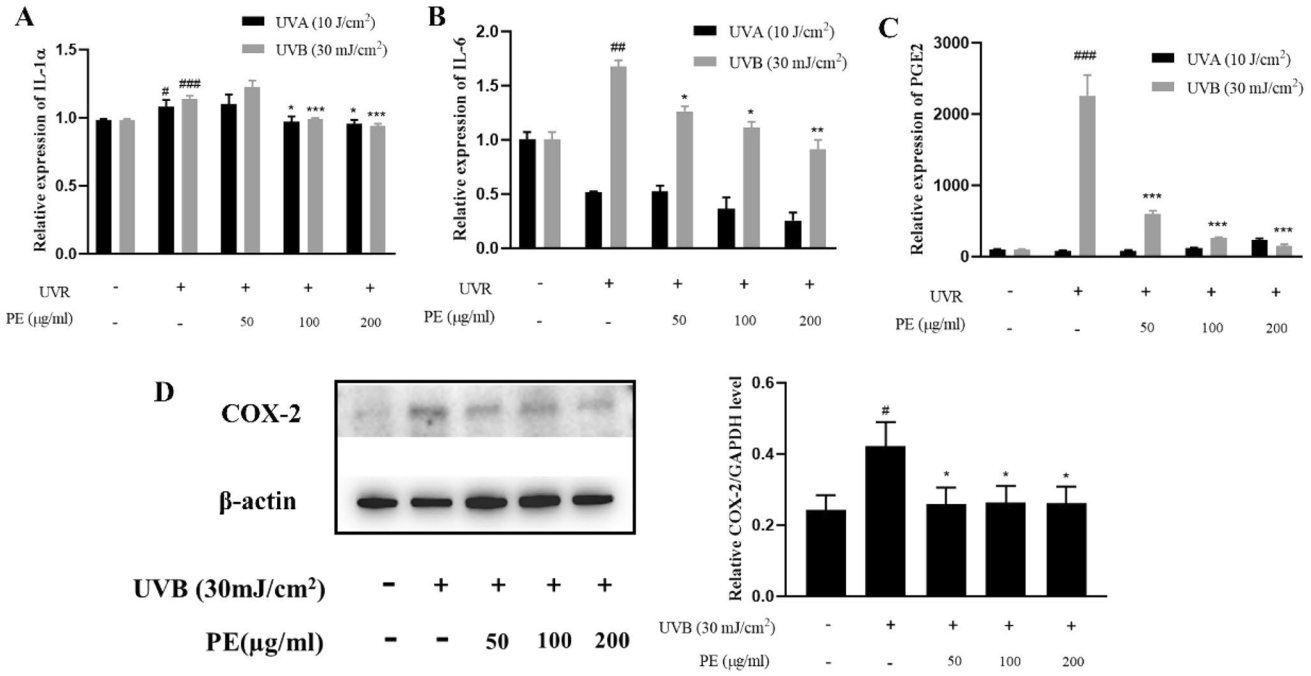

Fig. 4 The photoprotective effect of PE extract against the UVA and UVB induced inflammation. Relative productions of IL-1α (**A**), IL-6 (**B**) and PGE2 (**C**) after UVA (10 J/cm^2) and UVB exposure (30 mJ/cm^2) and pre-treatment with the different concentrations of PE extract were accessed by ELISA assay. **D** The western blot image analysis and relative activation analysis of COX-2 protein after UVB (30 mJ/cm^2) exposure and pre-treatment with the different concentrations of PE extract were measured by western blot assay. Significant differences were based on a one-way analysis of variance (ANOVA) and two-detailed *T*-test $^{\#}P<0.05$, $^{\#\#}P<0.01$ and $^{\#\#\#}P<0.001$ with respect to the blank group and $*P<0.05$, $**P<0.01$ and $***P<0.001$ with respect to UVR exposure group

in Supplement Table 2 and could be selected as targets for studying the protective mechanism of PE extract.

As shown in Fig. 5A, six genes (TCG) were chosen and determined by qRT-PCR, which were significantly regulated by UVA and UVB radiation. FOSB, JUN, EGR1, PTGS2, TNF, EGR1 and HMOX1 mRNA levels were elevated in UVR-irradiated HaCaT cells, which were significantly reduced upon pre-treatment with PE extract. These data suggested that these genes were simultaneously upregulated by UVA and UVB radiation. FOSB and Jun belong to the AP-1 family members, which are activated through the MAPK signaling pathway and TNF signaling pathway [22]. Shen et al. [23] discovered that EGR1 could be stimulated and induced by various cytokines and hormones through the MAPK/ERK1/2 signaling pathway, thereby regulating the expression of target genes, which caused cell differentiation, apoptosis, and other pathophysiological processes. TNF and PTGS2 are mainly involved in the TNF signaling pathway, which is an important pathway in the regulation of inflammation, apoptosis and cell survival as well as immunity [24]. The increased intracellular ROS level could upregulate the HMOX1 expression [25]. The experiments described above showed that UV irradiation might induce apoptosis, inflammation and oxidative stress of skin cells through TNF and MAPK signaling pathways. The addition of PE could suppress the activation of TNF and MAPK signaling pathways.

Besides, qRT-PCR was performed to evaluate the regulation of four genes (EGFR, CDC27, BUB1 and HSPA2) listed in TBG in Supplement Table 2. As shown in Fig. 5B, in the UVB-irradiated HaCaT cells, the expression levels of EGFR, CDC27 and BUB1 mRNA were significantly downregulated, which were reversed after PE pre-treatment. EGFR knockdown could induce cell-cycle arrest and apoptosis accompanied with a decrease of several EGFR downstream proteins [26]. CDC27 is a subunit of the anaphase-promoter complex, and its knockdown leads to cellular arrest in mitosis [27]. Then, Bub1 depletion causes apoptosis upon the imposition of mitotic arrest [28]. EGFR, CDC27 and BUB1 genes are associated with the cell cycle and apoptosis, which are involved in the MAPK signaling pathway. HSPA2 is an apoptosis-related gene that contributes to MAPK signaling [29]. Compared with the UVB-irradiated group, with the increase of PE concentration, the expression of HSPA2 mRNA decreased (Fig. 5B). These experimental results showed that UVB irradiation induced cell apoptosis, which led to skin injury.

Meanwhile, four genes listed in TAG of Supplement Table 2 were selected and assessed by qRT-PCR. As shown in Fig. 5C, increased levels of MMP3, MMP10 and

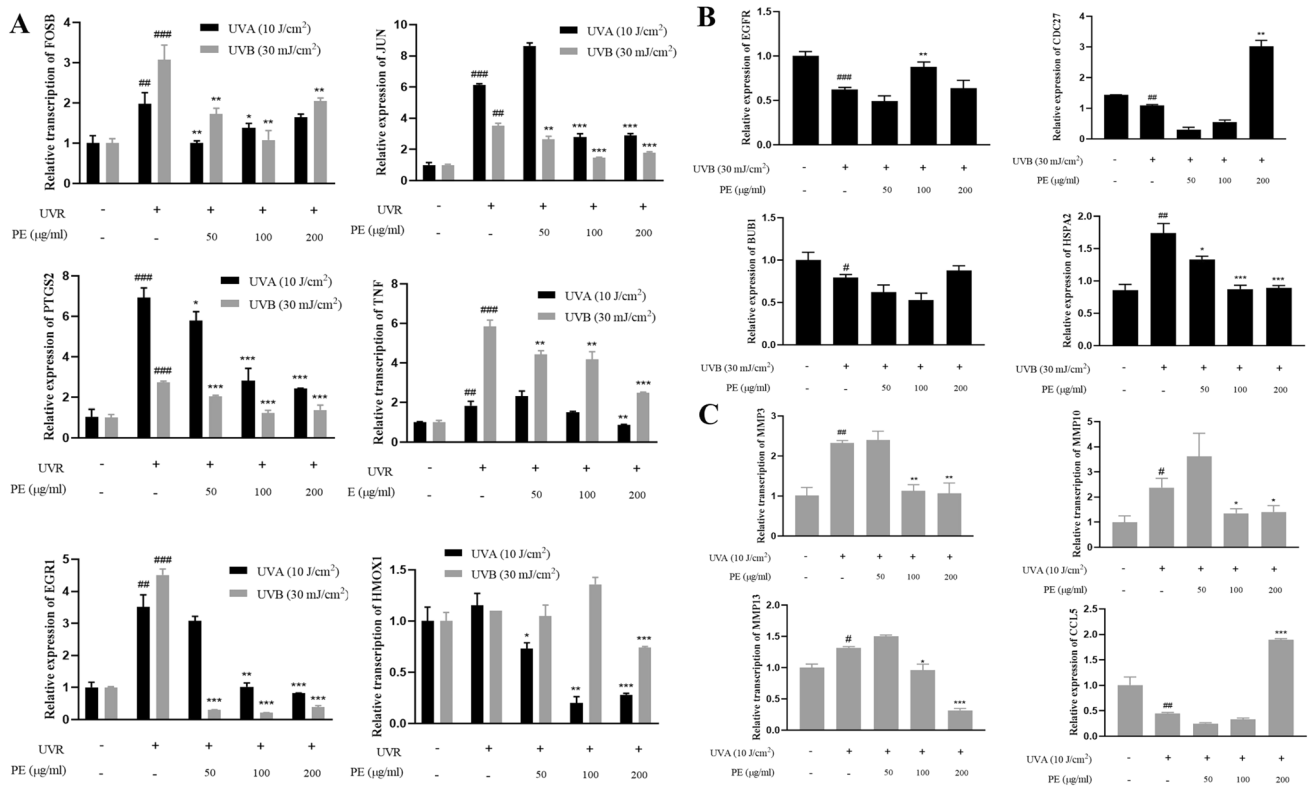

Fig. 5 Mechanism research of UVA and UVB induced HaCaT damage through differentially expressed genes analysis. (A) Relative expression of FOSB, JUN, PTGS2, TNF, EGR1 and HMOX1 mRNA after UVA (10 J/cm^2) and UVB exposure (30 mJ/cm^2) and pre-treatment with the different concentrations of PE extract was quantified by qRT-PCR. (B) Relative expression of EGFR, CDC27, BUB1 and PTGS2 mRNA after UVB exposure (30 mJ/cm^2) and pre-treatment with the different concentrations of PE extract was quantified by qRT-PCR. (C) Relative expression of MMP3, MMP10, MMP13 and CCL5 mRNA after UVA (10 J/cm^2) and pre-treatment with the different concentrations of PE extract was quantified by qRT-PCR. Significant differences were based on a one-way analysis of variance (ANOVA) and two-detailed *T*-test $^{\#}P<0.05$, $^{\#\#}P<0.01$ and $^{\#\#\#}P<0.001$ with respect to the blank group and $*P<0.05$, $**P<0.01$ and $***P<0.001$ with respect to UVR exposure group

MMP13 were found in HaCaT cells irradiated with UVA radiation. Photoaging of the skin is marked by atrophy of dermal connective tissue, which occurs as ECM components, particularly collagen fibers, are destroyed [30]. Keratinocytes and fibroblasts in the skin are stimulated to produce MMPs, including MMP-1, -2, -3, -9, and -13, which degrade collagen, elastin and other proteins [31]. The genes MMP3, MMP10 and MMP13 are involved in the TGF-β/Smad signaling pathway, which have the remodeling of ECM effect [32]. However, after 50, 100 and 200 μg/ml of PE pre-treatment, MMP3, MMP10 and MMP13 mRNA expressions were downregulated. This study confirmed that UVA considerably increased MMPs and induced skin photoaging. PE extract could alleviate the photoaging effect of UVA-radiation on the skin through decreasing the expression of MMPs.

3.7 Anti-apoptotic properties of PE extract through the inhibition of MAPK/AP-1 signaling pathway in UVB-irradiated HaCaT cells

From the results of the experiments described above, we knew that UVB irradiation could induce cell apoptosis. PARP1 and caspase-3 are apoptosis-related proteins that can reflect the degree of apoptosis. In the present study, exposure of HaCaT cells to UVB remarkably induced cleaved PARP1 and cleaved caspase-3 expression (Fig. 6A). It further demonstrated UVB-ray could promote cell apoptosis. However, the expression levels of cleaved PARP1 and cleaved caspase-3 were downregulated with 100 and 200 μg/ml of PE extract, which indicated that PE extract could relieve cell apoptosis induced by UVB irradiation (Fig. 6A).

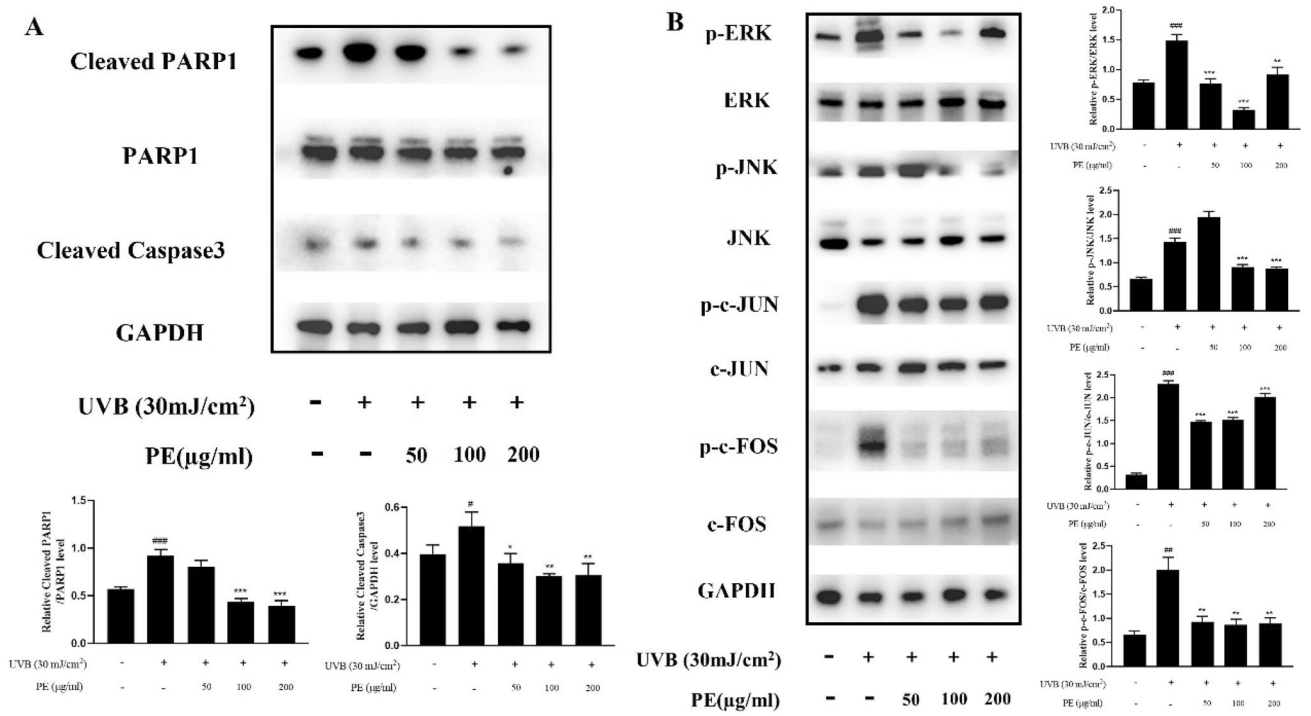

Fig. 6 The anti-apoptotic effect of PE extract against UVB irradiation through the inhibition of MAPK/AP-1 signaling pathway. **A** The western blot image analysis and relative activation analysis of apoptosis related proteins (Cleaved PARP1, PARP and Cleaved Caspase3) after UVB (30 mJ/cm^2) exposure and pre-treatment with the different concentrations of PE extract were measured by western blot assay. **B** The western blot image analysis and relative activation analysis of MAPK/AP-1 signaling pathway related proteins (p-ERK, ERK, p-JNK, JNK, p–c-JUN, c-JUN, p–c-FOS and c-FOS) after UVB (30 mJ/cm^2) exposure and pre-treatment with the different concentrations of PE extract were measured by western blot assay. Significant differences were based on a one-way analysis of variance (ANOVA) and two-detailed *T*-test $^{\#}P<0.05$, $^{\#\#}P<0.01$ and $^{\#\#\#}P<0.001$ with respect to the blank group and $^{*}P<0.05$, $^{**}P<0.01$ and $^{***}P<0.001$ with respect to UVR exposure group

The MAPK signaling pathway regulates apoptosis pathways [33]. Therefore, western blot analysis was performed to detect ERK, JNK, c-JUN and c-FOS phosphorylation. The steady expression of GAPDH was considered as an internal reference. As shown in Fig. 6B, the ratio of the phosphorylation of ERK to the expression of ERK gradually increased after UVB exposure, the phosphorylation of JNK was increased significantly in the group treated with UVB, the phosphorylated c-JUN and c-FOS were increased significantly. These results revealed that UVB treatment led to the activation of ERK, JNK, c-JUN and c-FOS, UVB-induced apoptosis might be mediated by the MAPK signaling pathways. Compared with the control group, the expression of phosphorylated JNK reduced in 100 and 200 μg/ml of PE pre-treatment group, the expression of phosphorylated ERK, c-JUN and c-FOS were decreased in the group of 50, 100 and 200 μg/ml PE significantly. These findings indicated that PE could protect keratinocytes from UVB-induced cell apoptosis through MAPK/AP-1 signaling pathway.

3.8 Anti-photoaging properties of PE extract through the activation of ERK/TGF-β/Smad signaling pathway in UVA-irradiated HaCaT cells

ECM such as collagen, fibronectin and elastin can be degraded by MMPs, resulting in photoaging [30]. Therefore, Elastin, Collagen I and Collagen III protein expressions were measured by western blot analysis. As shown in Fig. 7A, HaCaT cells treated with UVA radiation showed downregulation in the protein expressions of Elastin, Collagen I and Collagen III compared with non-irradiated cells. Pre-treatment with PE increased the protein expressions of Elastin, Collagen I and Collagen III in a dose-dependent manner. In particular, 200 μg/ml of PE elevated Elastin, Collagen I and Collagen III expression by 139.46%, 145.80%, and 75.64% compared to the irradiated group, respectively.

Transforming growth factor β (TGF-β) signaling is mediated via a Smad dependent pathway. After TGF receptors (TGF-RI and TGF-RII) are activated, Smads are phosphorylated and activated, resulting in regulation of extracellular

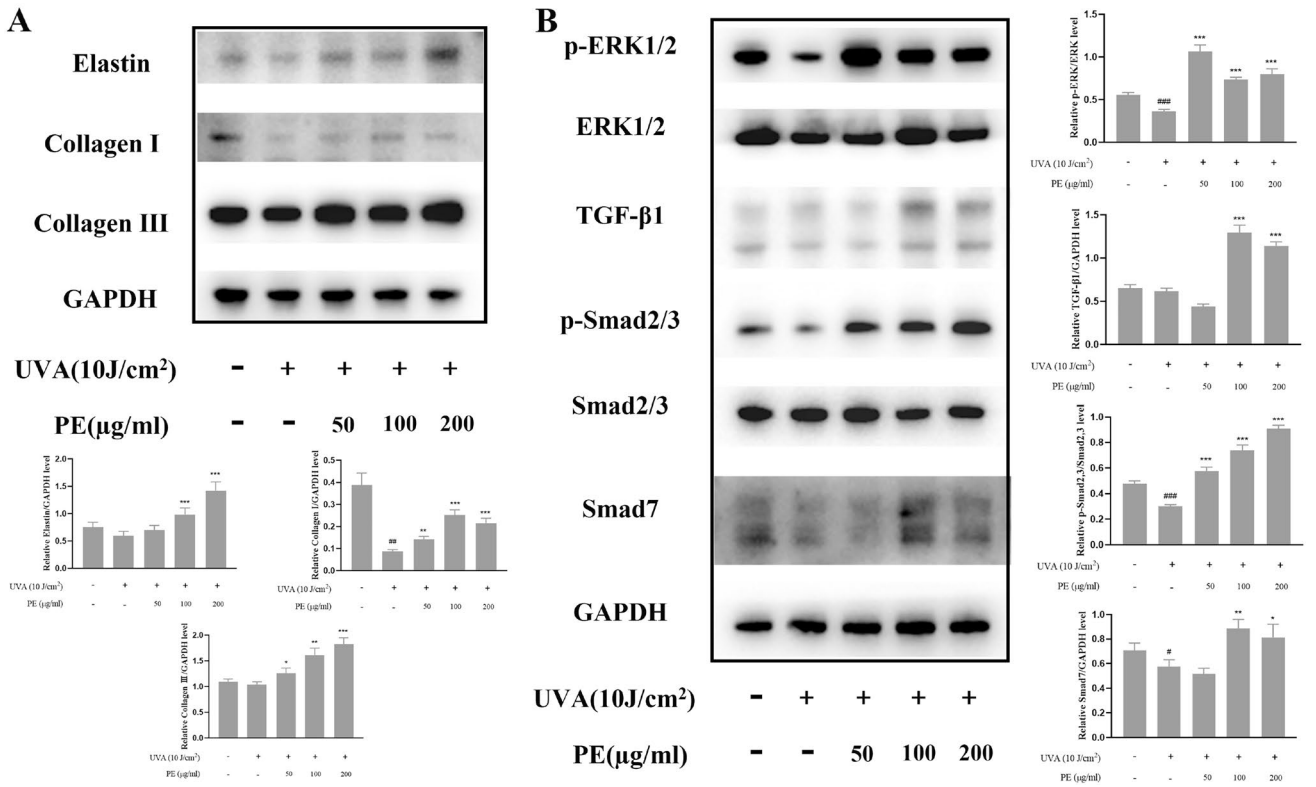

Fig. 7 The anti-photoaging effect of PE extract against UVA irradiation through the activation of ERK/TGF-β/Smad signaling pathway. **A** The western blot image analysis and relative activation analysis of ECM-associated proteins (Elastin, Collagen I and Collagen III) after UVA (10 J/cm^2) exposure and pre-treatment with the different concentrations of PE extract were measured by western blot assay. **B** The western blot image analysis and relative activation analysis of ERK/TGF-β/Smad signaling pathway related proteins (p-ERK1/2, ERK1/2, TGF-β1, p-Smad2/3, Smad2/3 and Smad7) after UVA (10 J/cm^2) exposure and pre-treatment with the different concentrations of PE extract were measured by western blot assay. Significant differences were based on a one-way analysis of variance (ANOVA) and two-detailed T-test $^{\#}P<0.05$ and $^{\#\#\#}P<0.001$ with respect to the blank group and $*P<0.05$, $**P<0.01$ and $***P<0.001$ with respect to UVR exposure group

matrix proteins, including fibronectin, collagen, and MMPs [32]. At the same time, ERK phosphorylation can also be activated by TGF-β [34]. Western blot analysis was performed to identify whether exposure to UVA stimulated ERK/TGF-β/Smad signaling pathway. Our results demonstrated that phosphorylated ERK, TGF-β1, phosphorylated Smad2/3 and Smad7 were downregulated following exposure to UVA (10 J/cm^2). Moreover, this result was reversed by PE pre-treatment (Fig. 7B). The levels of phosphorylated ERK, TGF-β1, phosphorylated Smad2/3 and Smad7 were decreased when compared to UVA-exposed cells. Taken together, these results indicated that UVA irradiation could inhibit ERK/TGF-β/Smad signaling pathway to induce photoaging and PE exerted anti-photoaging effect by ERK/TGF-β/Smad signaling pathway.

4 Discussion

Skin damage is primarily caused by chronic and excessive exposure of UV radiation from sunlight, especially UVA and UVB, which causes sunburn, photocarcinogenesis, photosensitive reaction, immune suppression and photoaging on skin [35]. The UVB radiation damages DNA directly, which can result in skin reddening, sunburn and apoptosis [36]. The UVA makes up more than 90% of the ultraviolet radiation reaching the earth's surface and contributes to skin aging and wrinkles due to damage to cellular DNA by producing ROS [37]. Human keratinocytes, as the outermost layer of the skin, are the first responders to

UV radiation. It has been demonstrated that UV irradiation can induce keratinocytes to undergo apoptosis, autophagy, inflammatory and aging. In laboratory studies, the doses of UVA and UVB radiation given to cultured cells are typically higher than the ambient levels of these types of radiation that would be encountered during normal sun exposure. We chose 10 J/cm^2 of UVA or 30 mJ/cm^2 UVB as irradiation dose based on the previous study [21], which have shown that 10 J/cm^2 of UVA or 30 mJ/cm^2 UVB can cause cell damage and decrease cell survival rates without causing excessive harm and affecting cell growth status.

Based on our previous research, the combination of transcriptomic and proteomic analyses in our work revealed common and differential genes or proteins in human primary keratinocytes exposed to UVA and UVB [21]. By combing protein–protein interactions (PPI) and molecular complex detection method (MCODE) analyses, hub genes or proteins were discovered in each group, which could be the basis for subsequent research on the mechanism of skin damage caused by UV radiation. Moreover, UVB and UVA radiation significantly influenced the transcription of 983 genes by analysis of DEGs, which were defined as TCG. Then 7191 genes were identified specifically in UVB irradiated cells, which were classified as TBG group. At the same time, there were 458 genes being specifically expressed in UVA irradiated cells, which were designed TAG group. As shown in Supplement Table 2, clustering analysis and selection of hub genes with high node degrees were carried out using Cytoscape software of MCODE and Cytohubba. The most enriched TCG functional modules were associated with biological processes, including ubiquitin-dependent protein catabolic process, G-protein coupled receptor, inflammatory response and cell division. In TBG group, the most enriched functional modules majorly participated in protein ubiquitination, cell division and DNA repair. And the most enriched modules in TAG were mainly involved in type I interferon signaling pathway, extracellular matrix disassembly, chemotaxis and inflammatory response.

It is well known that the fruit of PE, as a rich source of phenolics, has antioxidant, anti-inflammatory, antimicrobial and hypoglycemic activities [38]. According to the Chinese Pharmacopoeia, the quality standard for PE extract is based on the content of gallic acid, hence we determined the gallic acid and total polyphenol levels of the PE extract and found that they met the requirements specified in the Pharmacopoeia. As one of the important phenolic compounds in PE extract, gallic acid can serve as one of the pharmacological activities for the efficacy of PE extract. In this study, the contents of polyphenols and gallic acid of PE were $41.61 \pm 1.82\%$ and $2.15 \pm 0.11\%$, respectively. Khwandow reported that the treatment of skin keratinocytes with PE extract relieved the UVB-induced oxidative stress and apoptosis through scavenging of ROS [13]. But there are few reports on the mechanism research of PE against photo-damage induced by UVA and UVB, respectively. In the present study, PE extract had the ability to prevent damage of keratinocyte cells induced by UV light. To explore the photoprotective mechanism of PE, fourteen hub DEGs were selected from TCG, TBG and TAG groups as potential targets for functional and pathway signaling studies caused by UV radiation. QRT-PCR results showed that PE could exert the photoprotective effect via inflammatory inhibition, DNA repair and regulation of MAPK signaling pathway exposed to UVB. Meanwhile, PE could play the anti-photoaging effect through anti-inflammatory, suppressing ECM degeneration and regulation of ERK/TGF-β/Smad signaling pathway with UVA-irradiated.

ROS are accumulated in response to UV radiation and these interfere with the function of the macromolecules, such as lipids, proteins, and DNA, resulting in cell death, apoptosis and DNA damage [39]. Our results revealed that the PE greatly suppressed both UVA and UVB induced excessive production of ROS. The production of ROS and free radicals caused by UV light eventually led to cell death via necrosis. Meanwhile, it is wildly known that UV, especially UVB, is a potent inducer of apoptosis [40]. In our study, both UVA and UVB irradiation caused necrosis of keratinocytes, but UVB was the dominant factor in early apoptosis compared to UVA. Meanwhile, long-term exposure of UV light leads to sustaining oxidative stress which can induce skin photoaging by promoting MMPs synthesis and collagen degradation [41]. Our results showed an oxidative stress in HaCaT cells induced by UVA radiation affecting both MMPs synthesis and antioxidant enzyme (HO-1 and SOD1) activities.

The interleukin-1 alpha (IL-1α), a member of interleukin 1 family, possesses potent proinflammatory effect and induces extracellular matrix degradation [42]. And it can trigger the activation of a serious of signaling pathways through linking the cell surface receptor, IL-1R1. Furthermore, UV irradiation can strongly promote the expression of proinflammatory cytokine IL-6 in keratinocytes, which IL-6 also modulates stratum corneum regeneration and skin barrier function [43]. PGE2, as one of proinflammatory mediators, enhanced microvascular permeability of endothelial membrane through the induction of VEGF which leads to swelling and redness pain on skin [44]. Arachidonic acid (AA) is converted by COX2 into PGE2, which is positively regulated by COX2, and COX2 expression may be increased upon the accumulation of PGE2 [20]. In our study, both UVA and UVB irradiation induced inflammatory responses. However, exposure of UVB light could impair the skin-barrier, cause redness, swell and induce acute inflammatory response than UVA.

There are three parallel pathways in the Mitogen-activated protein kinase (MAPK) family, ERK/MAPK, JNK/MAPK and p38/MAPK. The MAPK pathway is a key

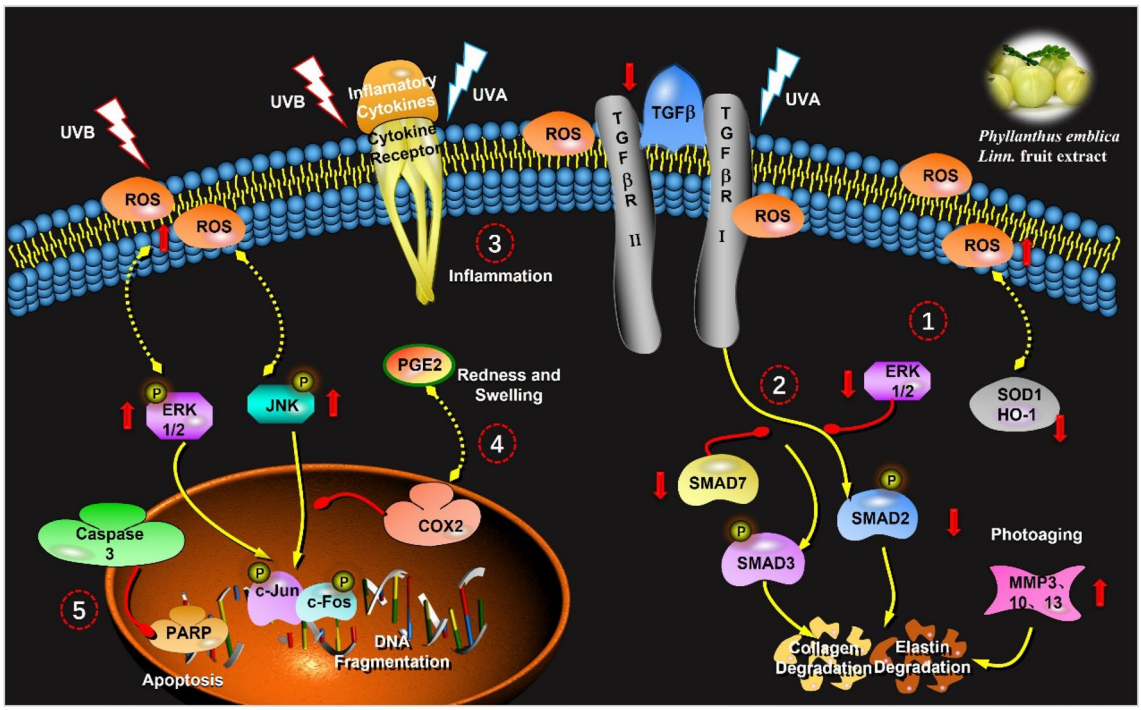

Fig. 8 Schematic summary illustrating the corresponding molecular mechanisms of UVA and UVB induced HaCaT cell damage. (1) UVA-induced oxidative stress generated excessive reactive oxygen species (ROS) and reduced the levels of antioxidant enzymes. (2) UVA exposure inhibited the ERK/TGF-β/Smad signaling pathway, which led to degradation of elastin and collagen and caused skin photoaging. (3) UVA and UVB irradiation drived the release of inflammatory factors, resulting in skin inflammation. (4) UVB increased COX-2 expression and PGE2 production was upregulated, which caused skin redness and swelling. (5) Exposure of UVB induced cell apoptosis through activation of the MAPK/AP-1 signaling pathway. Pre-treatment of PE extract expressed photoprotective effects against UVA and UVB on the five pathways discussed above

pathway regulating cellular function, particularly MAPK/ERK, which plays a key role in cell proliferation, differentiation, survival and apoptosis [45]. Our results manifested that UVB radiation could promote oxidative stress and inflammation by increasing ROS production and proinflammatory factor releases, as well as upregulate phosphorylation of ERK, JNK, c-JUN and c-FOS, suggesting that the MAPK/AP-1 signaling pathway in keratinocyte was activated and regulated apoptosis induced by UVB. The apoptotic cleavage products of PARP1 and caspase 3 were suppressed by pre-treatment with PE extract upon UVB irradiation and PE extract contributed to activation of the MAPK/AP-1 signaling pathway in HaCaT cells. Thus, the anti-apoptotic effect of PE extract was exerted via the MAPK/AP-1 signaling pathway.

Photoaging is significantly accelerated in the skin by UVA-ray, which leads to cell senescence and ECM damage [46]. The TGF-β/Smad pathway can regulate the ECM protein secretion, cell proliferation and cell cycle progression. In this study, exposure of UVA could reduce the phosphorylation of ERK, which can be rapidly activated by TGF-β1. Moreover, the TGF-β/Smad signaling pathway was inhibited and elastin and collagen synthesis was affected by UVA, which is responsible for the skin's structural support and the resilience. Hence, UVA radiation was a major cause of skin photoaging through inhibiting ERK/TGF-β/Smad signaling pathway. PE extract exerted the anti-photoaging effect by the activation of ERK/ TGF-β/Smad signaling pathway.

Our findings revealed that UVA and UVB light cause skin cell injury via different mechanisms and pathways (Fig. 8). It provided us appropriate strategies for alleviating UV-damage to the skin. PE extract could play photo-protective and anti-photoaging roles via MAPK/AP-1 signaling pathway and ERK/ TGF-β/Smad signaling pathway (Fig. 8). This work revealed that PE extract, a traditional food and medicinal plant, can be considered as a good and safe candidate for oral and topical photoprotection preparations against harmful UV radiation. Research on PE extract has demonstrated its potential utility in natural healthcare products, such as food, health, and cosmetic products [47, 48]. There is some evidence that suggests PE extract can have a positive impact on the skin, such as anti-aging, skin whitening and antioxidant properties [47, 49, 50]. However, more research is needed to fully understand the effects of PE extract on the skin and its optimal use as a topical treatment.

Electronic supplementary material The online version of this article (https://doi.org/10.1007/s43630-023-00423-3) contains supplementary material, which is available to authorized users.

Acknowledgements The authors gratefully acknowledge funding from independent research fund of Yunnan Characteristic Plant Extraction Laboratory (2022YKZY001 and 2022YKZY003).

Author contributions YC and LQ designed the experiments. LQ performed the experiments and analyzed the data. YC and FW wrote the paper. All authors discussed and approved the final manuscript.

Data availability The original contributions generated for this study are included in the article/supplementary material, further inquiries can be directed to the corresponding author/s.

Declarations

Conflict of interest The authors declare no competing financial interest.

References

1. Wang, H., Wang, Y., Fu, F., Qian, Y., Xiao, Y., Yang, D., & Qiu, X. (2020). Controlled preparation of lignin/titanium dioxide hybrid composite particles with excellent UV aging resistance and its high value application. *International Journal of Biological Macromolecules, 150*, 371–379.
2. Svobodova, A., Walterova, D., & Vostalova, J. (2006). Ultraviolet light induced alteration to the skin. *Biomedical Papers, 150*, 25–28.
3. Muthusamy, V., & Piva, T. J. (2010). The UV response of the skin: A review of the MAPK, NFκB and TNFα signal transduction pathways. *Archives of Dermatological Research, 302*, 5–17.
4. Gallagher, R. P., & Lee, T. K. (2006). Adverse effects of ultraviolet radiation: a brief review. *Progress in Biophysics and Molecular Biology, 92*, 119–131.
5. Cezar, T. L., Martinez, R. M., Rocha, C. D., Melo, C. P., Vale, D. L., Borghi, S. M., Fattori, V., Vignoli, J. A., Camilios-Neto, D., & Baracat, M. M. (2019). Treatment with maresin 1, a docosahexaenoic acid-derived pro-resolution lipid, protects skin from inflammation and oxidative stress caused by UVB irradiation. *Scientific Reports, 9*, 1–14.
6. Wenk, J., Brenneisen, P., Meewes, C., Wlaschek, M., Peters, T., Blaudschun, R., Ma, W., Kuhr, L., Schneider, L., & Kochanek, K. S. (2001). UV-induced oxidative stress and photoaging. *Current Problems in Dermatology, 29*, 83–94.
7. Kunkel, G. H., Chaturvedi, P., & Tyagi, S. C. (2016). Mitochondrial pathways to cardiac recovery: TFAM. *Heart Failure Review, 21*, 499–517.
8. Danovaro, R., Bongiorni, L., Corinaldesi, C., Giovannelli, D., Damiani, E., Astolfi, P., Greci, L., & Pusceddu, A. (2008). Sunscreens cause coral bleaching by promoting viral infections. *Health Perspectives, 116*, 441–447.
9. Parrado, C., Philips, N., Gilaberte, Y., Juarranz, A., & Gonzalez, S. (2018). Oral photoprotection: effective agents and potential candidates. *Frontiers in Medicine, 5*, 188–206.
10. Zhang, T., Huang, S., Qiu, J., Wu, X., Yuan, H., & Park, S. (2022). Beneficial effect of gastrodia elata blume and poria cocos wolf administration on acute UVB irradiation by alleviating inflammation through promoting the gut-skin axis. *International Journal of Molecular Sciences, 23*, 10833–10859.
11. Heinrich, U., Neukam, K., Tronnier, H., Sies, H., & Stahl, W. (2006). Long-term ingestion of high flavanol cocoa provides photoprotection against UV-induced erythema and improves skin condition in women. *Journal of Nutrition, 136*, 1565–1569.
12. Gonzalez, S., Pathak, M., Cuevas, J., Villarrubia, V., & Fitzpatrick, T. (1997). Topical or oral administration with an extract of *Polypodium leucotomos* prevents acute sunburn and psoralen-induced phototoxic reactions as well as depletion of Langerhans cells in human skin. *Photodermatology, Photoimmunology and Photomedicine, 13*, 50–60.
13. Kunchana, K., Jarisarapurin, W., Chularojmontri, L., & Wattanapitayakul, S. K. (2021). Potential use of amla (*Phyllanthus emblica* L.) fruit extract to protect skin keratinocytes from inflammation and apoptosis after UVB irradiation. *Antioxidants, 10*, 703–721.
14. Kaur, S., & Muthuraman, A. (2019). Ameliorative effect of gallic acid in paclitaxel-induced neuropathic pain in mice. *Toxicology Reports, 6*, 505–513.
15. Zhou, Y. D., Fang, X. F., & Cui, Z. J. (2009). UVA-induced calcium oscillations in rat mast cells. *Cell Calcium, 45*, 18–28.
16. Bae, J. S., Han, M., Shin, H. S., Kim, M. K., Shin, C. Y., Lee, D. H., & Chung, J. H. (2017). Perilla frutescens leaves extract ameliorates ultraviolet radiation-induced extracellular matrix damage in human dermal fibroblasts and hairless mice skin. *Journal of Ethnopharmacology, 195*, 334–342.
17. Fortes, G. B., Alves, L. S., Oliveira, R. D., Dutra, F. F., Rodrigues, D., Fernandez, P. L., Padron, T. S., De Rosa, M. J., Kelliher, M., & Golenbock, D. (2012). Heme induces programmed necrosis on macrophages through autocrine TNF and ROS production. *Blood, 119*, 2368–2375.
18. Yu, X., Zhao, Q., Zhang, H., Fan, C., Zhang, X., Xie, Q., Xu, C., Liu, Y., Wu, X., & Han, Q. (2016). Gambogenic acid inhibits LPS-simulated inflammatory response by suppressing NF-κB and MAPK in macrophages. *Acta Biochimica et Biophysica Sinica, 48*, 454–461.
19. FitzGerald, G., & Ricciotti, E. (2011). Prostaglandins and inflammation. *Arteriosclerosis, 31*, 986–1000.
20. Obermajer, N., & Kalinski, P. (2012). Key role of the positive feedback between PGE2 and COX2 in the biology of myeloid-derived suppressor cells. *Oncoimmunology, 1*, 762–764.
21. Zhao Q, Chen Y, Qu L (2022) Combined Transcriptomic and proteomic analyses reveal the different responses to UVA and UVB radiation in human Keratinocytes. Photochemistry and Photobiolog 1–16
22. Plotnikov, A., Zehorai, E., Procaccia, S., & Seger, R. (1813). The MAPK cascades: signaling components, nuclear roles and mechanisms of nuclear translocation. *Acta - Molecular Cell Research, 2011*, 1619–1633.
23. Delmastro, M. M., & Piganelli, J. D. (2011). Oxidative stress and redox modulation potential in type 1 diabetes. *Clinical and Developmental Immunology, 2011*, 1–15.
24. Kumar, P., Natarajan, K., & Shanmugam, N. (2014). High glucose driven expression of pro-inflammatory cytokine and chemokine genes in lymphocytes: molecular mechanisms of IL-17 family gene expression. *Cellular Signalling, 26*, 528–539.
25. Shono, Y., Tuckett, A. Z., Liou, H. C., Doubrovina, E., Derenzini, E., Ouk, S., Tsai, J. J., Smith, O. M., Levy, E. R., & Kreines, F. M. (2016). Characterization of a c-Rel inhibitor that mediates anticancer properties in hematologic malignancies by blocking NF-κB–controlled oxidative stress responses. *Cancer Research, 76*, 377–389.
26. Liu, H., Lu, J., Hua, Y., Zhang, P., Liang, Z., Ruan, L., Lian, C., Shi, H., Chen, K., & Tu, Z. (2015). Targeting heat-shock protein 90 with ganetespib for molecularly targeted therapy of gastric cancer. *Cell Death & Disease, 6*, e1595–e1595.
27. Kittler, R., Putz, G., Pelletier, L., Poser, I., Heninger, A. K., Drechsel, D., Fischer, S., Konstantinova, I., Habermann, B., &

Grabner, H. (2004). An endoribonuclease-prepared siRNA screen in human cells identifies genes essential for cell division. *Nature, 432*, 1036–1040.
28. Yamada, H., & Rao, C. (2010). Genes that modulate the sensitivity for anti-microtubule drug-mediated chemotherapy. *Current Cancer Drug Targets, 10*, 623–633.
29. Gurunathan, S., Qasim, M., Park, C. H., Iqbal, M. A., Yoo, H., Hwang, J. H., Uhm, S. J., Song, H., Park, C., & Choi, Y. (2019). Cytotoxicity and transcriptomic analyses of biogenic palladium nanoparticles in human ovarian cancer cells (SKOV3). *Nanomaterials, 9*, 787–810.
30. Kim, J., Lee, C. W., Kim, E. K., Lee, S. J., Park, N. H., Kim, H. S., Kim, H. K., Char, K., Jang, Y. P., & Kim, J. W. (2011). Inhibition effect of Gynura procumbens extract on UV-B-induced matrix-metalloproteinase expression in human dermal fibroblasts. *Journal of Ethnopharmacology, 137*, 427–433.
31. Quan, T., Qin, Z., Xia, W., Shao, Y., Voorhees, J. J., & Fisher, G. J. (2009). Matrix-degrading metalloproteinases in photoaging. *Journal of Investigative Dermatology Symposium Proceedings, 14*, 20–24.
32. Verrecchia, F., Chu, M. L., & Mauviel, A. (2001). Identification of novel TGF-β/Smad gene targets in dermal fibroblasts using a combined cDNA microarray/promoter transactivation approach. *Journal of Biological Chemistry, 276*, 17058–17062.
33. Wada, T., & Penninger, J. M. (2004). Mitogen-activated protein kinases in apoptosis regulation. *Oncogene, 23*, 2838–2849.
34. Zhang, Y. E. (2017). Non-Smad signaling pathways of the TGF-β family. *Cold Spring Harbor Perspectives in Biology, 9*, a022129–a022149.
35. Wang, S. Q., Stanfield, J. W., & Osterwalder, U. (2008). In vitro assessments of UVA protection by popular sunscreens available in the United States. *Journal of the American Academy of Dermatology, 59*, 934–942.
36. Wang, S. Q., Balagula, Y., & Osterwalder, U. (2010). Photoprotection: a review of the current and future technologies. *Dermatologic Therapy, 23*, 31–47.
37. Zou, W., González, A., Jampaiah, D., Ramanathan, R., Taha, M., Walia, S., Sriram, S., Bhaskaran, M., Dominguez-Vera, J. M., & Bansal, V. (2018). Skin color-specific and spectrally-selective naked-eye dosimetry of UVA, B and C radiations. *Nature Communications, 9*, 1–10.
38. Perianayagam, J. B., Sharma, S., Joseph, A., & Christina, A. (2004). Evaluation of anti-pyretic and analgesic activity of *Emblica officinalis* Gaertn. *Journal of Ethnopharmacology, 95*, 83–85.
39. Mrakic-Sposta, S., Gussoni, M., Vezzoli, A., Dellanoce, C., Comassi, M., Giardini, G., Bruno, R. M., Montorsi, M., Corciu, A., & Greco, F. (2020). Acute effects of triathlon race on oxidative stress biomarkers. *Oxidative Medicine and Cellular Longevity, 2020*, 1–14.
40. Kuechle, M. K., & Elkon, K. B. (2017). Shining light on lupus and UV. *Arthritis Research and Therapy, 9*, 1–3.
41. Xiao, Y., Ren, Q., & Wu, L. (2022). The pharmacokinetic property and pharmacological activity of acteoside: a review. *Biomedicine & Pharmacotherapy, 153*, 113296–113309.
42. Huguier, V., Giot, J. P., Simonneau, M., Levillain, P., Charreau, S., Garcia, M., Jégou, J. F., Bodet, C., Morel, F., & Lecron, J. C. (2019). Oncostatin M exerts a protective effect against excessive scarring by counteracting the inductive effect of TGFβ1 on fibrosis markers. *Scientific Reports, 9*, 1–10.
43. Wang, X. P., Schunck, M., Kallen, K. J., Neumann, C., Trautwein, C., Rose-John, S., & Proksch, E. (2004). The interleukin-6 cytokine system regulates epidermal permeability barrier homeostasis. *Journal of Investigative Dermatology, 123*, 124–131.
44. Funk, C. D. (2001). Prostaglandins and leukotrienes: advances in eicosanoid biology. *Science, 294*, 1871–1875.
45. Torres, M., & Forman, H. J. (2003). Redox signaling and the MAP kinase pathways. *BioFactors, 17*, 287–296.
46. Xiao, X., Wu, Z. C., & Chou, K. C. (2011). A multi-label classifier for predicting the subcellular localization of gram-negative bacterial proteins with both single and multiple sites. *PLoS One, 6*, e20592–e20602.
47. Chaikul, P., Kanlayavattanakul, M., Somkumnerd, J., Lourith, N. J. J. O. T., & Medicine, C. (2021). *Phyllanthus emblica* L. (amla) branch: a safe and effective ingredient against skin aging. *Journal of Traditional and Complementary Medicine, 11*, 390–399.
48. Bandyopadhyay, S. K., Pakrashi, S. C., & Pakrashi, A. J. J. O. E. (2000). The role of antioxidant activity of *Phyllanthus emblica* fruits on prevention from indomethacin induced gastric ulcer. *Journal of Ethnopharmacology, 70*, 171–176.
49. Majeed, M., Bhat, B., Anand, S., Sivakumar, A., Paliwal, P., & Geetha, K. G. (2011). Inhibition of UV-induced ROS and collagen damage by *Phyllanthus emblica* extract in normal human dermal fibroblasts. *Journal of Cosmetic Science, 62*, 49–57.
50. Lin, Y. Y., Lu, S. H., Gao, R., Kuo, C. H., Chung, W. H., Lien, W. C., Wu, C. C., Diao, Y., Wang, H.-M.D.J.O.M., & Longevity, C. (2021). A novel biocompatible herbal extract-loaded hydrogel for acne treatment and repair. *Oxidative Medicine and Cellular Longevity, 2021*, 1–13.